Supplementary Information

Osmotic Coefficient and Mean Ionic Activity Coefficient of Supersaturated Ammonium Nitrate Solutions Measured by Laser Trapping and Raman Spectroscopy

Kento Kuniyoshi[a] and Shoji Ishizaka[a,*]

[a] *Graduate School of Advanced Science and Engineering, Hiroshima University, 1-3-1 Kagamiyama, Higashi-Hiroshima 739-8526, Japan*

* Corresponding author:

Shoji Ishizaka − ORCID ID: 0000-0001-9866-5809

Graduate School of Advanced Science and Engineering, Hiroshima University, 1-3-1 Kagamiyama, Higashi-Hiroshima 739-8526, Japan

E-mail: ishizaka@hiroshima-u.ac.jp

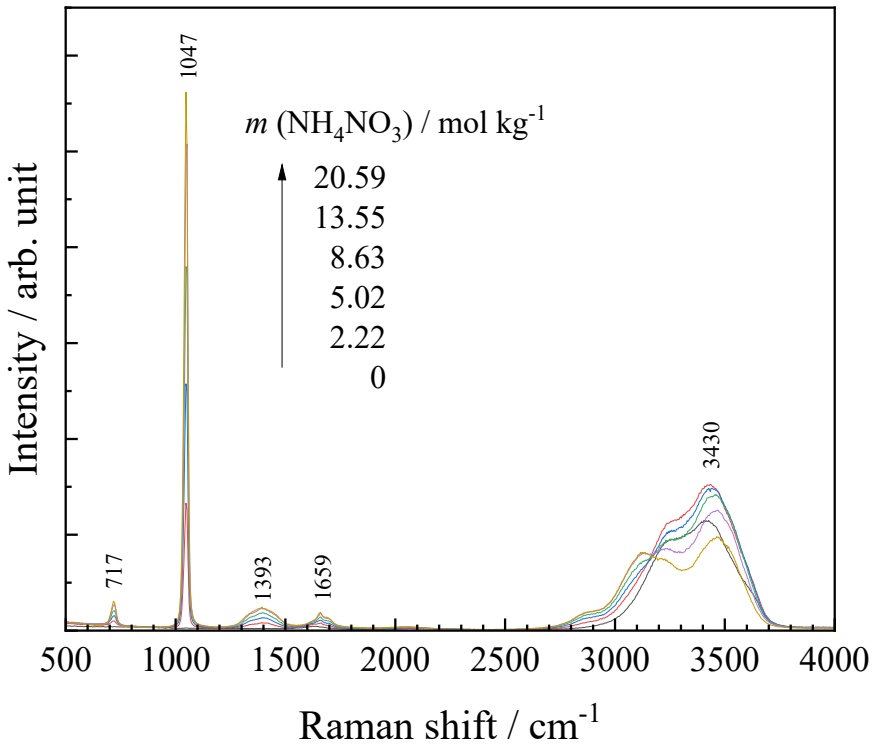

Fig. S1 Concentration dependence of the Raman spectra of bulk aqueous NH_4NO_3 solutions.

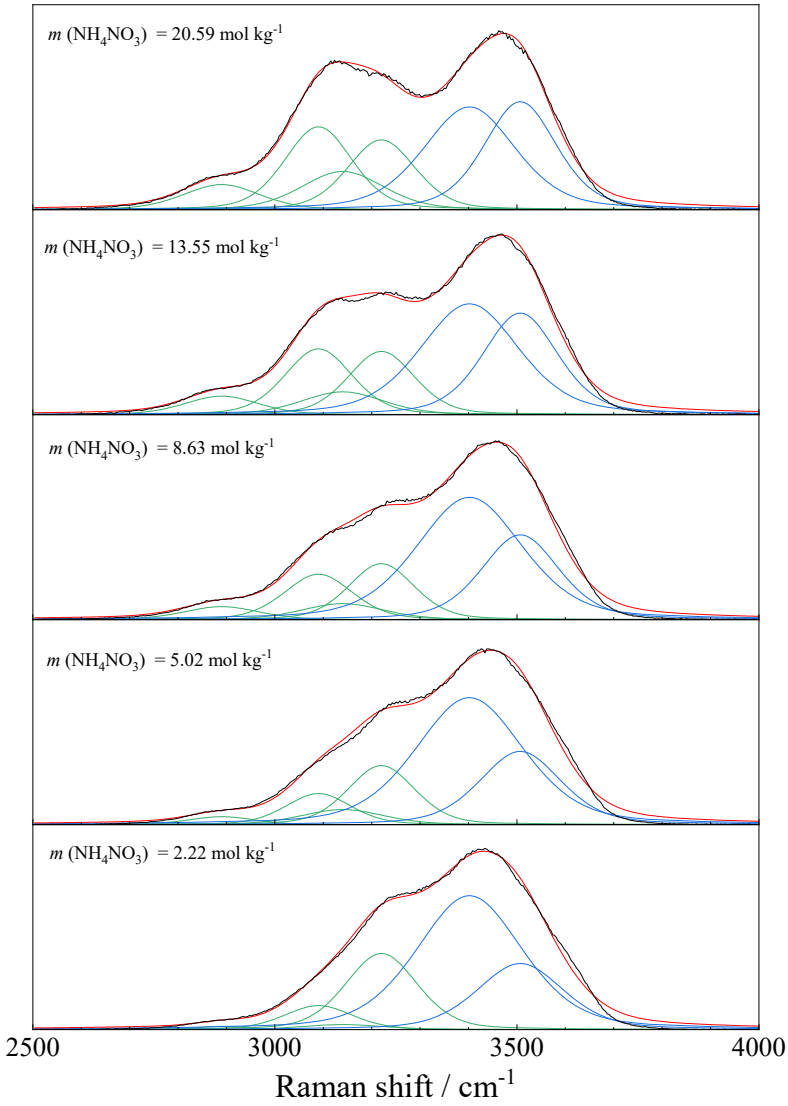

Fig. S2 Peak-deconvolution fitting of the Raman spectra (2500–4000 cm^{-1}) of bulk aqueous NH_4NO_3 solutions, with x_c (center wavenumbers) at 2890, 3090, 3140, 3220, 3402, and 3507 cm^{-1}.

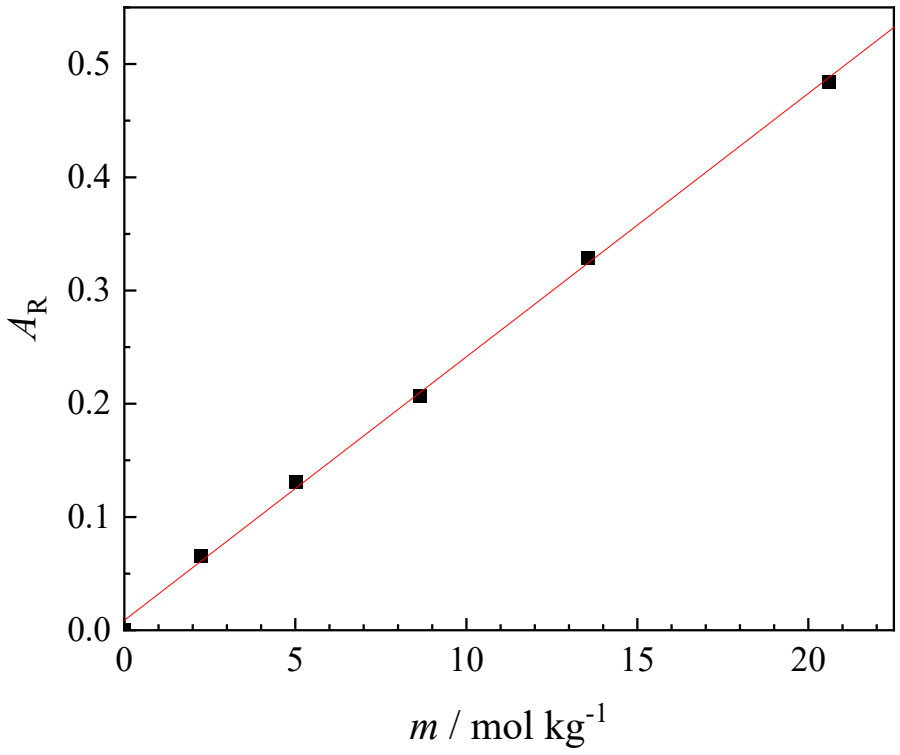

Fig. S3 Dependence of the area ratio (A_R), defined as the peak area at 1047 cm^{-1} relative to the sum of the peak areas at 3402 and 3507 cm^{-1}, on the molality of NH_4NO_3. The solid line shows a linear least-squares regression fit (slope = 0.023 ± 0.001 kg mol^{-1}; intercept = 0.01 ± 0.01; R^2 = 0.999).

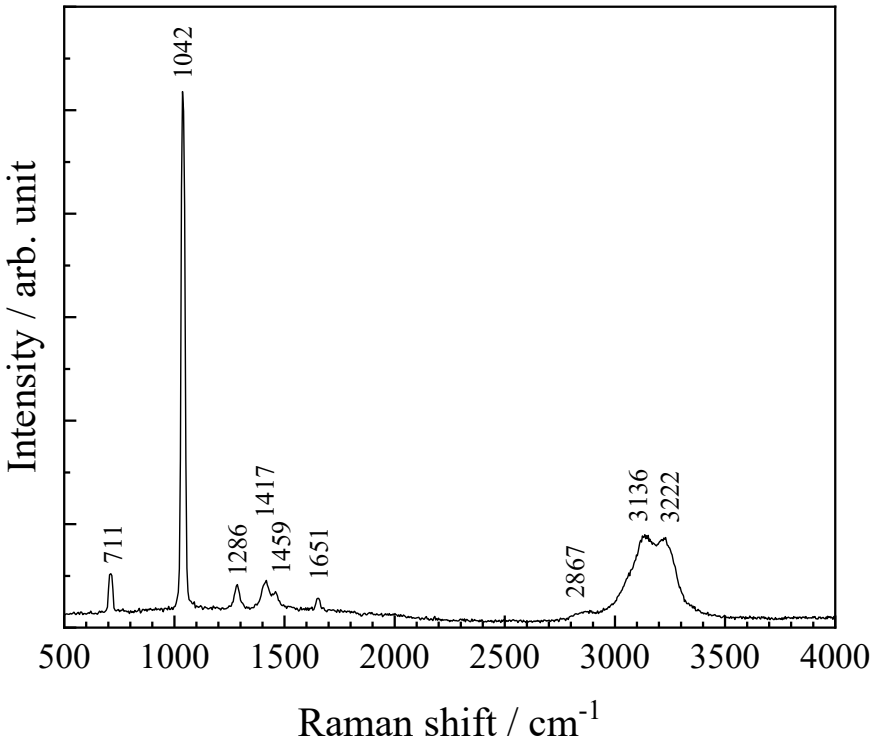

Fig. S4 Raman spectrum of NH_4NO_3 crystals.

Table S1. Raman-spectroscopy-derived and image-based droplet-volume-interpolated thermodynamic data for the optically levitated aqueous NH_4NO_3 droplet corresponding to the solid-circle symbols in Figs. 5–7, measured at 25.0 ± 0.5 °C and ambient pressure (≈1 atm).

a_w	V / 10^{-12} L	n / 10^{-11} mol	C_s mol L^{-1}	d g cm^{-3}	m mol kg^{-1}	x_I	ϕ	$\gamma_{\pm}$
0.850	3.22	1.66	5.16	1.153	**7.0**	0.201	0.644	0.264
0.840	3.02	1.66	5.50	1.163	7.6	0.215	0.637	0.255
0.836	2.93	1.66	5.69	1.168	8.0	0.223	0.621	0.246
0.832	2.93	1.66	5.69	1.168	8.0	0.223	0.638	0.250
0.811	2.62	1.66	6.35	1.187	9.4	0.252	0.619	0.231
0.795	2.47	1.66	6.73	1.198	10.2	0.269	0.624	0.225
0.785	2.36	1.66	7.06	1.207	11.0	0.284	0.611	0.216
0.773	2.25	1.66	7.40	1.217	11.9	0.299	0.601	0.207
0.722	1.97	1.66	8.41	1.245	**14.7**	0.346	0.615	0.193
0.699	1.80	1.66	9.26	1.268	17.6	0.388	0.565	0.171
0.680	1.73	1.66	9.66	1.278	19.0	0.406	0.563	0.165
0.673	1.70	1.66	9.76	1.282	20.0	0.413	0.550	0.159
0.665	1.66	1.66	10.03	1.289	20.6	0.426	0.550	0.157
0.647	1.64	1.66	10.11	1.245	**21.0**	0.431	0.575	0.160
0.593	1.45	1.66	11.48	1.328	28.0	0.503	0.518	0.132
0.559	1.37	1.66	12.16	1.346	32.6	0.540	0.495	0.120
0.543	1.33	1.66	12.48	1.355	35.1	0.558	0.483	0.114
0.534	1.32	1.66	12.66	1.360	36.5	0.568	0.477	0.111
0.528	1.32	1.66	12.66	1.360	36.5	0.568	0.486	0.112
0.523	1.31	1.66	12.71	1.361	**37.0**	0.571	0.486	0.111
0.503	1.28	1.66	13.03	1.369	39.9	0.590	0.478	0.106
0.473	1.22	1.66	13.59	1.384	45.9	0.623	0.453	0.096
0.467	1.22	1.66	13.63	1.385	46.3	0.625	0.456	0.096
0.462	1.20	1.66	13.82	1.390	48.7	0.637	0.440	0.092
0.459	1.20	1.66	13.82	1.390	48.7	0.637	0.444	0.092
0.450	1.19	1.66	14.02	1.395	51.2	0.649	0.433	0.089
0.441	1.19	1.66	14.03	1.396	51.4	0.649	0.442	0.089
0.434	1.17	1.66	14.22	1.401	54.1	0.661	0.428	0.086
0.429	1.17	1.66	14.25	1.402	54.5	0.663	0.431	0.085
0.426	1.15	1.65	14.35	1.405	**56.0**	0.669	0.423	0.083

0.396	1.13	1.65	14.61	1.411	60.5	0.685	0.425	0.080
0.383	1.12	1.65	14.79	1.416	63.7	0.696	0.418	0.077
0.360	1.10	1.65	15.06	1.424	**69.0**	0.713	0.411	0.073
0.319	1.07	1.65	15.46	1.433	78.9	0.740	0.402	0.067
0.306	1.05	1.65	15.70	1.440	85.7	0.755	0.384	0.062
0.287	1.05	1.65	15.73	1.441	86.8	0.758	0.399	0.063
0.270	1.02	1.63	15.96	1.447	**94.0**	0.772	0.387	0.059
0.222	1.00	1.63	16.23	1.454	105	0.791	0.398	0.056
0.201	0.99	1.63	16.49	1.460	117	0.809	0.381	0.051
0.168	0.96	1.61	16.82	1.468	**138**	0.833	0.359	0.045
0.142	0.94	1.61	17.12	1.477	161	0.853	0.336	0.040
0.125	0.94	1.61	17.12	1.477	161	0.853	0.358	0.041
0.102	0.93	1.61	17.39	1.484	189	0.872	0.335	0.036
0.079	0.91	1.60	17.57	1.488	**215**	0.886	0.328	0.033

a_w; the activity of water.

V (L); the droplet volume determined by image analysis, assuming a spherical droplet.

n (mol); the amount of NH_4NO_3 in the droplet.

C_s (mol L^{-1}); The molar concentration of NH_4NO_3 in the droplet.

d (g cm^{-3}); the density of the aqueous NH_4NO_3 solution, calculated using the parameterization reported by Clegg *et al.* (*J. Phys. Chem A*, 2011, 115, 3393-346).

m (mol kg-1); the molality of NH_4NO_3.

x_I; the total ionic mole fraction calculated by Eq. (3) in the main text.

ϕ; the osmotic coefficient, calculated from the measured water activity a_w using Eq. (7).

$\gamma_{\pm}$; the mean molal ionic activity coefficient, obtained from numerical integration of the Gibbs–Duhem equation using Eq. (10).

The molality values shown in **__**bold and underlined text**__** correspond to values directly estimated from Raman spectral deconvolution analysis and are identical to those listed in Table 1 of the main text.

All other molality values were obtained by interpolation based on image-derived droplet volume changes between successive Raman measurements, followed by conversion from molar concentration to molality using the coresponding density values.

Table S2. Thermodynamic properties of additional optically levitated aqueous NH_4NO_3 droplets corresponding to the star symbols in Figs. 5–7, measured at 25.0 ± 0.5 °C and ambient pressure (≈1 atm)..

a_w	V / 10^{-12} L	n / 10^{-11} mol	C_s mol L^{-1}	d g cm^{-3}	m mol kg^{-1}	x_I	ϕ	$\gamma_\pm$
0.832	4.00	2.28	5.70	1.168	8.0	0.224	0.638	0.248
0.828	3.94	2.28	5.79	1.171	8.2	0.228	0.640	0.247
0.826	3.88	2.28	5.88	1.173	8.4	0.232	0.635	0.243
0.815	3.65	2.28	6.25	1.184	9.2	0.248	0.620	0.232
0.804	3.48	2.28	6.56	1.193	9.8	0.261	0.616	0.225
0.789	–	–	–	–	**9.5**	0.256	–	–
0.789	3.21	2.28	7.11	1.208	11.1	0.286	0.591	0.209
0.788	3.16	2.28	7.23	1.212	11.4	0.292	0.579	0.204
0.766	2.95	2.28	7.73	1.226	12.7	0.314	0.581	0.195
0.748	2.76	2.28	8.27	1.241	14.3	0.340	0.564	0.183
0.720	2.62	2.28	8.72	1.253	15.7	0.361	0.581	0.178
0.710	2.48	2.28	9.19	1.266	17.3	0.384	0.549	0.165
0.670	2.27	2.28	10.06	1.290	20.8	0.428	0.535	0.150
0.651	2.14	2.28	10.64	1.306	23.4	0.458	0.508	0.138
0.625	2.07	2.28	11.05	1.317	25.6	0.480	0.510	0.132
0.569	1.80	2.18	12.09	1.345	32.1	0.536	0.487	0.115
0.542	1.77	2.18	12.34	1.351	33.9	0.550	0.501	0.114
0.523	1.71	2.18	12.72	1.361	**37.1**	0.572	0.485	0.107
0.510	1.66	2.18	13.11	1.371	40.7	0.594	0.460	0.099
0.456	1.56	2.17	13.88	1.392	49.4	0.640	0.441	0.088
0.434	1.50	2.13	14.21	1.401	54.0	0.660	0.429	0.082
0.367	1.38	2.06	14.97	1.421	67.3	0.708	0.413	0.071
0.338	1.32	2.02	15.34	1.430	75.7	0.732	0.398	0.065
0.315	1.29	2.02	15.68	1.439	85.2	0.754	0.376	0.060
0.252	1.26	2.02	16.03	1.448	97.2	0.778	0.394	0.056
0.233	1.20	1.97	16.36	1.457	111	0.800	0.364	0.050
0.228	1.18	1.93	16.40	1.458	**113**	0.802	0.364	0.049
0.169	1.15	1.93	16.78	1.468	134	0.829	0.367	0.044
0.120	1.12	1.93	17.17	1.478	166	0.857	0.355	0.038

Definitions of a_w, V, n, C_s, d, m, x_I, ϕ, and $\gamma_\pm$ are identical to those given in Table S1.
The molality values shown in **<u>**bold and underlined text**</u>** correspond to values directly estimated from Raman spectral deconvolution analysis.

For molalities $m \leq 25.6\ \mathrm{mol\ kg^{-1}}$, only a single Raman spectrum was available at each concentration, and the resulting molality values were systematically lower than the corresponding literature values. Therefore, in this concentration range, the molality m was estimated with reference to the E-AIM model.

In the concentration range between m = 37.1 and 113 $\mathrm{mol\ kg^{-1}}$, the spacing of molality values directly obtained from Raman spectroscopy was relatively large. Therefore, the amount of solute n in this range was estimated with reference to the solid-circle data listed in Table S1.

The final two data points (m = 134 and 166 $\mathrm{mol\ kg^{-1}}$) were obtained by extrapolation rather than interpolation. These values lie within the molality range covered by the solid-circle data listed in Table S1, and their magnitudes are consistent with the corresponding thermodynamic trends observed therein. On this basis, the extrapolated values were considered to be physically reasonable and are included here.

Table S3. Thermodynamic properties of additional optically levitated aqueous NH_4NO_3 droplets corresponding to the diamond symbols in Figs. 5–7, measured at 25.0 ± 0.5 °C and ambient pressure (≈1 atm)..

a_w	V / 10^{-12} L	n / 10^{-11} mol	C_s mol L^{-1}	d g cm^{-3}	m mol kg^{-1}	x_I	ϕ	$\gamma_\pm$
0.682	2.48	2.48	9.99	1.288	**<u>20.5</u>**	0.424	0.519	0.153
0.658	2.44	2.48	10.17	1.293	21.2	0.434	0.547	0.155
0.632	2.31	2.48	10.74	1.308	23.9	0.463	0.532	0.144
0.598	2.19	2.48	11.30	1.323	**<u>27.0</u>**	0.493	0.529	0.136
0.561	2.07	2.47	11.96	1.341	31.2	0.529	0.515	0.125
0.529	1.95	2.47	12.67	1.360	36.6	0.569	0.483	0.112
0.513	1.88	2.45	13.06	1.370	40.2	0.592	0.460	0.104
0.501	1.88	2.41	12.86	1.365	**<u>38.3</u>**	0.580	0.501	0.111
0.444	1.66	2.35	14.13	1.398	52.8	0.656	0.427	0.087
0.419	1.63	2.35	14.42	1.406	57.3	0.674	0.422	0.082
0.409	1.60	2.32	14.53	1.409	59.1	0.681	0.420	0.081
0.341	1.50	2.29	15.27	1.429	74.2	0.728	0.403	0.069
0.326	1.47	2.26	15.40	1.432	77.3	0.736	0.403	0.068
0.309	1.41	2.18	15.48	1.434	**<u>79.4</u>**	0.741	0.411	0.067
0.248	1.35	2.18	16.17	1.452	102	0.787	0.378	0.056

Definitions of a_w, V, n, C_s, d, m, x_I, ϕ, and $\gamma_\pm$ are identical to those given in Table S1.

The molality values shown in ****<u>bold and underlined text</u>**** correspond to values directly estimated from Raman spectral deconvolution analysis.

All other molality values were obtained by interpolation based on image-derived droplet volume changes between successive Raman measurements, followed by conversion from molar concentration to molality using the coresponding density values.

The final data point (m = 102 mol kg^{-1}) was obtained by extrapolation rather than interpolation. This value lies within the molality range covered by the data in Table S1, and its magnitude is consistent with the corresponding thermodynamic trends observed for the solid-circle data. On this basis, the extrapolated value was considered to be physically reasonable and is included here.